# Constraints on Early Events in Martian History as Derived From the Cratering Record

NADINE G. BARLOW[1]

*Lunar and Planetary Institute, Houston, Texas*

The shapes and densities of crater size-frequency distribution curves are used to constrain two major events early in Martian history: termination of high obliteration rates and viability of the multiple impact origin of the crustal dichotomy. Distribution curves of fresh craters superposed on uplands, intercrater plains, and ridged plains display shapes and densities indicative of formation prior to the end of heavy bombardment. This observation correlates with other geologic evidence, suggesting a major change in the erosional regime following the last major basin size impact (i.e., Argrye). In addition, the multisloped nature of the curves supports the idea that the downturn in the crater size-frequency distribution curves reflects the size-frequency distribution of the impactors rather than being the result of erosion. The crustal dichotomy formed prior to the heavy bombardment intermediate epoch based on distribution curves of knobby terrain; if the dichotomy resulted from a single gigantic impact, this observation places constraints on when this event happened. An alternate theory for dichotomy formation, the multiple-impact basin idea, is questioned: since distribution curves of large basins as well as heavy bombardment era units are not represented by a -3 differential power law function, this study finds fewer basins missing on Mars compare to the Moon and Mercury than previously reported. The area covered by these missing basins is less than that covered the northern plains.

## INTRODUCTION

Analysis of Mariner 9 and Viking imagery has revealed that the Martian surface experienced a variety of geologic processes throughout its history. However, despite almost two decades of study, much of the early history of Mars remains unknown. Since processes operating during the first billion years of Martian history (e.g., formation of the crustal dichotomy) have affected the subsequent geologic evolution of the planet, it is important to understand the timing and origin of these processes if we wish to unravel the history of Mars. Origins of these processes are theorized based on geologic interpretation and geophysical modeling: for example, the crustal dichotomy has been attributed to both internal [*Wise et al.*, 1979] and impact [*Wilhelms and Squyres*, 1984; *Frey and Schultz*, 1988a] processes. The timing of these early events can be constrained by analysis of the impact cratering record preserved in ancient terrains. This report discusses the implications of the cratering record on two events occurring early in Martian history: the viability of the multiple-impact origin of the crustal dichotomy and the cessation time of the high obliteration rates which occurred during the period of late heavy bombardment.

## INTERPRETATION OF THE CRATERING RECORD

Two techniques for the display of crater statistical data have been recommended by the *Crater Analysis Techniques Working Group* [1978]: cumulative and relative plots. The cumulative plot is the most common method used for displaying crater size-frequency distribution data but suffers

from a damping of the frequency variation amplitudes due to its cumulative nature. The relative or $R$ plot technique avoids this problem by only considering the number of craters within a particular diameter range. Since frequency variations are important in the analysis of the cratering record, the relative plotting technique will be used exclusively in this discussion.

Although relative plots are one of the two recommended techniques for the display of crater size-frequency distribution data, they are less commonly used than cumulative plots. Since comprehension of the discussion which follows depends on one's understanding of the $R$ plot technique and terminology, a short explanation is useful at this point. The $R$ plot is a differential plotting technique of the form

$$dN = kD^{-\beta} dD$$

where $k$ is a constant, $\beta$ is the differential population or slope index (which is equal to the cumulative slope plus one), $dN$ is the number of craters within the diameter range $dD$ (often $\sqrt{2}$ diameter-sized increments, but not always), and $D$ is the diameter. The $R$ plot normalizes to a differential -3 (cumulative or incremental -2) slope, so that any distribution curve approximating a differential power law function of -3 slope will appear as a horizontal line on this plot. Thus variations from a power law distribution function are readily apparent as changes in slope on the $R$ plot. To use this technique, one plots log $R$ versus log $D$, where $R$ is a parameter given by

$$R = N\bar{D}^{-3}/[A(Db - Da)]$$

$N$ is the number of craters within the diameter range $D_a$ to $D_b$ ($D_b = D_a \sqrt{2}$), $\bar{D}$ is the geometric mean of the diameter bin ($= \sqrt{D_a D_b}$), and $A$ is the area over which the craters are counted.

Figure 1 shows relative crater size-frequency distribution plots for terrains on the Moon, Mercury, and Mars. Two

---
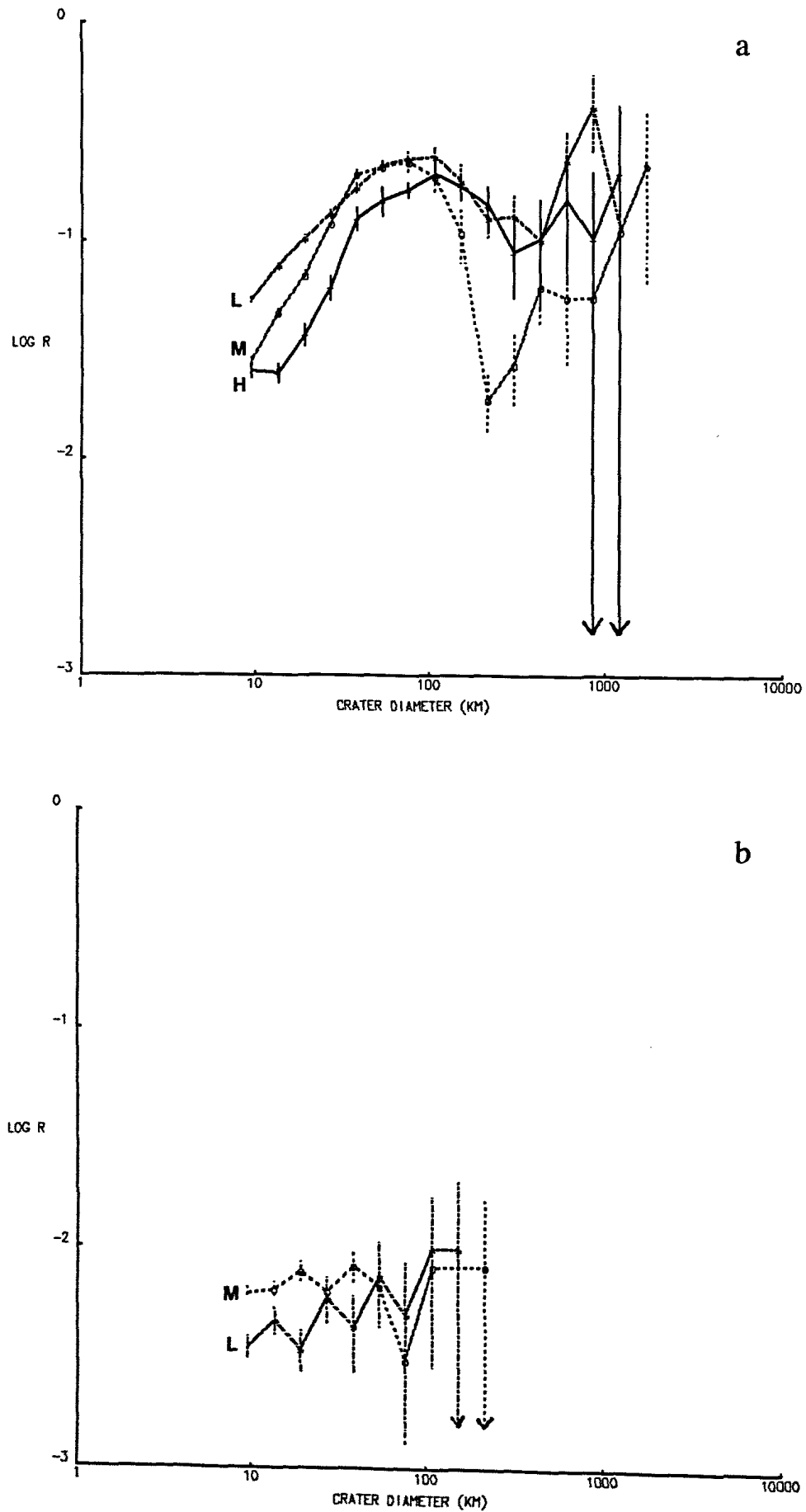
Fig. 1. Relative crater size-frequency distribution plots of terrain units on the Moon (L), Mercury (H), and Mars (M). (a) Distribution curves of the heavily cratered regions of the Moon, Mercury and Mars. (b) Distribution curves of the lunar mare and Martian northern plains.

distinct types of curves are seen: the heavily cratered regions of all three objects display a multisloped distribution curve (Figure 1a) whereas the lunar mare and Martian northern plains show a flat curve which can be approximately by a power law function with differential slope -3 (equivalent to a -2 slope on a cumulative plot) (Figure 1b). The shapes of the three curves in Figure 1a are statistically identical to each other, and the two curves in Figure 1b are identical. However, the curves in Figure 1a are statistically different from those in Figure 1b at the 99% confidence level [Woronow et al., 1982; Barlow, 1988a]. The fact that heavily cratered regions cannot be represented by a single slope distribution function at all crater diameters has important implications for understanding the early history of the Moon, Mercury, and Mars.

Three theories exist to explain these different curve shapes: saturation [Hartmann, 1984], erosional effects [Neukum and Wise, 1976; Neukum and Hiller, 1981], and different production populations [Strom and Whitaker, 1976; Oberbeck et al., 1977]. Crater saturation broadly refers to the situation where a surface is so heavily cratered that all subsequent impacts simply overlap existing craters (see discussion by Basaltic Volcanism Study Project, [1981, pp. 1054-1063]). One result of crater saturation is no change in overall crater density. Of more importance to crater analysis, however, is the fact that no information about the size-frequency distribution of the production population can be obtained from a saturated surface and thus little age information can be derived. Although much controversy still exists regarding the prevalence of crater saturation conditions throughout the solar system [cf. Hartmann, 1984; Chapman and McKinnon, 1986], we believe the computer simulations by Woronow [1977, 1978, 1985] and observational evidence by Strom, Neukum, and their associates [Strom, 1977; Neukum, 1985; Barlow, 1988a] are strong arguments against saturation being the cause of the slope variations in the crater size-frequency distribution curves of heavily cratered regions at diameters ≥ 8 km.

The second theory, which explains the downturn in the lunar, Mercurian, and Martian highlands curve shape at diameters <70 km as primarily the result of erosion, also is contraindicated because this implies that obliterative processes have worked in tandem to obliterate craters less than about 70 km on all three bodies. This seems unlikely since these three worlds have different obliterative environments and have experienced very different thermal histories: one expects that erosion/deposition would cause the downturn to be observed at different crater diameters on the different bodies. The small variations in the diameter corresponding to the "peak" of the lunar, Mercurian, and Martian curves are consistent with decreasing impact velocity at increasing heliocentric distances (R. G. Strom, personal communication, 1988). Obliteration does affect the shape of the crater size-frequency distribution curves because of the preferential destruction of small craters (for example, the steep slope associated with the size-frequency distribution curves of mercurian craters less than about 70 km diameter is attributed to destruction of small craters by intercrater plains formation [Woronow et al., 1982], but we believe that these effects are superposed on an originally multisloped distribution function. New evidence supporting the idea that obliteration is not entirely responsible for the downturn observed in R plots of heavily cratered terrains will be

discussed later in the section on erosional processes in early Martian history.

We interpret the two statistically distinct crater size-frequency distribution curves in terms of the third theory that the shape of the curve is reflective of the size-frequency distribution of two different production populations. The multiple-sloped curve seen in heavily cratered regions is believed to record the size-frequency distribution of heavy bombardment era impactors. The flatter curve seen in the lunar mare and Martian plains represents impactors emplaced more recently, in the post-heavy bombardment period. The change in shape among the curves occurs around a log R value of -2 for both the Moon and Mars. Using this technique, Barlow [1987a; 1988a] revised the Martian relative chronology by noting the shape and density of size-frequency distribution curves associated with different geologic units (Figure 2). Table I lists the relative ages of major geologic units as derived in this chronology. This technique classifies approximately 60% of Martian terrain units into "heavy bombardment" (such as the intercrater plains of the southern highlands, the knobby terrain in the northern hemisphere, most of the highland patera, and the dissected terrain along the highlands/lowlands boundary) or "end of heavy bombardment" (where curves show multisloped characteristics but with a density near a value of log $R = -2$) (examples are the ridged plains (e.g., Lunae Planum, Syrtis Major, etc.) and the floors of the Hellas and Argyre Basins). The remaining 40% of terrain units show curves indicative of terrain formation in the post-heavy bombardment period (which includes much of the sparsely cratered northern plains). This chronology serves as the basis for the subsequent discussion of events acting over localized regions of Mars.

## EARLY OBLITERATIVE ENVIROMENT ON MARS

The existence of channels, volcanoes, and eolian features indicates that Mars has experienced a more active erosional history than either the Moon or Mercury, and this fact is recorded in the cratering record. A large number of craters in the Martian southern highlands are rimless and display shallow floors (Figure 3). Most investigators attribute this morphology to higher obliteration rates resulting from a thicker atmosphere early in Martian history [Sagan et al., 1973; Chapman, 1974; Pollack et al., 1987], although Squyres and Carr [1986] have suggested that viscous creep of terrain underlain by ground ice is responsible for these and other features at high latitudes. However, other geologic evidence (i.e., valley network location almost exclusively in ancient terrain) and experimental results (i.e., atmosphere isotopic data) support the idea that enhanced obliteration in the Martian past was at least partially responsible for the degradation seen in the highlands.

Several studies have estimated the timing of the obliteration event(s) responsible for the degradation of craters in the southern highlands. Öpik [1966] and Chapman et al. [1969] noted that crater data from Mariner 4 imagery did not follow a $D^{-2}$ power law function at diameters ≤30 km. They suggested that a constant obliteration rate had acted over all of Martian history, completely obliterating older craters ≤30 km in diameter and severely degrading recently formed craters in the same size range. Based on analyses of Mariner 6 and 7 crater data, several investigators suggested that erosional activity was high early in Martian history but
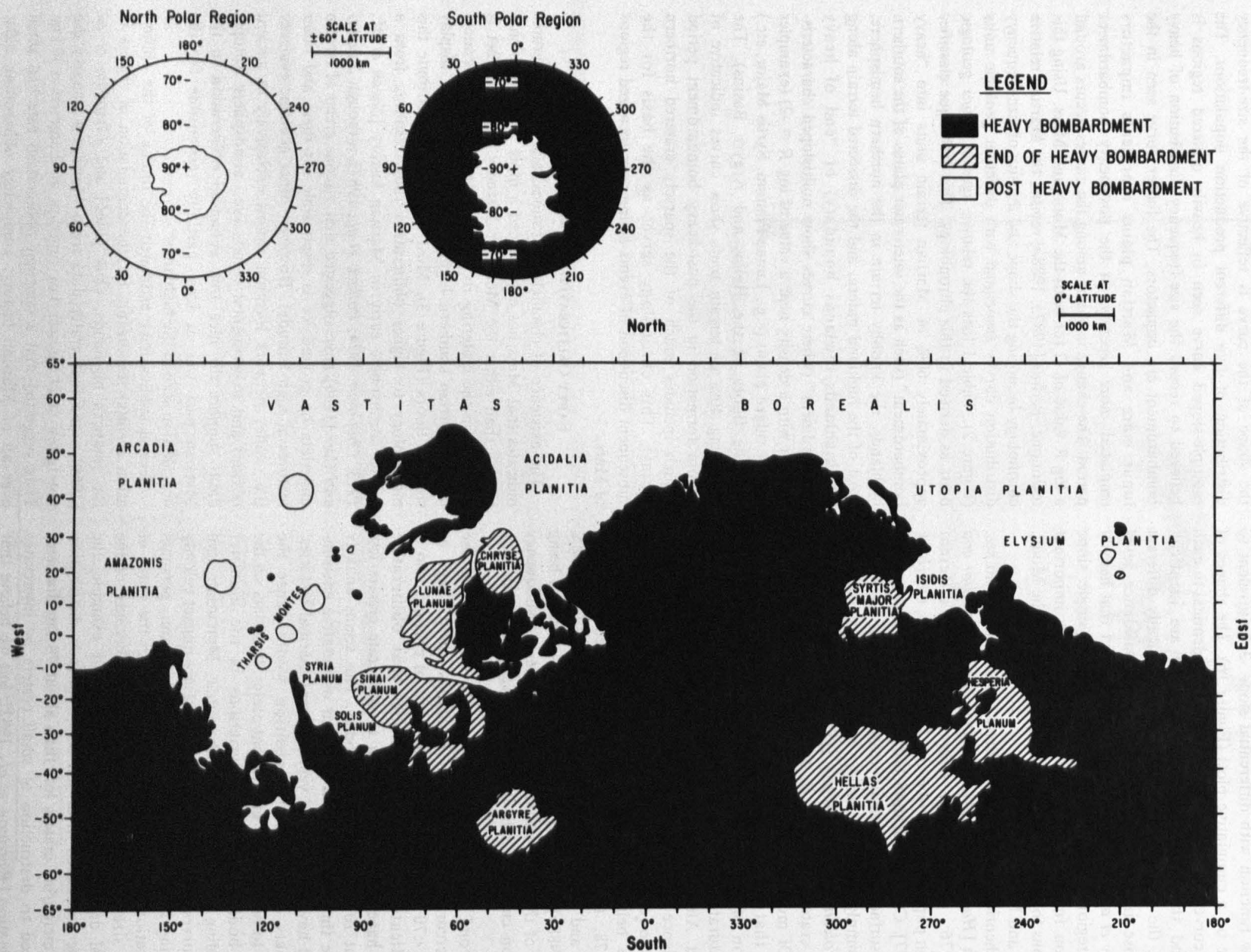
Fig. 2. Generalized chronology map for Mars derived from analysis of the shapes and densities of relative crater size-frequency distribution plots for 23 geologic units. After *Barlow* [1988a].

TABLE 1. Relative Ages of Terrain Units

| Unit | Area, $10^6$ km$^2$ | Average Crater Density | Age* |
|---|---|---|---|
| Uplands | 8.81 | 413 | HB |
| Intercrater plains | 46.8 | 217 | HB |
| Mountain | 3.00 | 269 | HB |
| Fractured uplands | 1.96 | 190 | HB |
| Fretted | 1.31 | 181 | HB |
| Exhumed uplands | 0.98 | 163 | HB |
| Dissected | 2.40 | 140 | HB |
| Knobby | 3.18 | 135 | HB |
| Hellas Volcanic | 1.36 | 116 | HB |
| Ridged plains | 8.85 | 82 | EHB |
| Cratered and fractured plains | 5.17 | 55 | PHB |
| Chaotic | 0.85 | 49 | PHB |
| Plains | 27.0 | 49 | PHB |
| Mottled plains | 10.6 | 37 | PHB |
| Equatorial layered deposits | 1.79 | 23 | PHB |
| Volcanic plains | 8.37 | 18 | PHB |
| Canyon floor | 1.10 | 9 | PHB |

*HB, heavy bombardment; EHB, end of heavy bombardment; PHB, post heavy bombardment.

has decreased substantially in intensity in recent times so that young craters are not as degraded as older craters [*Murray et al*, 1971; *Hartmann*, 1971; *McGill and Wise*, 1972; *Hartmann*, 1973]. *Soderblom et al.* [1974], using Mariner 9 data, correlated high obliteration rates with high cratering flux early in Martian history. Alternately, Chapman and Jones [*Chapman*, 1974; *Jones*, 1974; *Chapman and Jones*, 1977] concluded that moderate-sized craters (10-30 km

diameter) experienced a pulse of high obliteration rates subsequent to the early period of cratering when the impact flux was high. Studies of regional erosional history are being conducted using Viking imagery, particularly in the Martian plains [*Frey et al.*, 1988; *Maxwell and McGill*, 1988], but a global reanalysis similar to those of Chapman's and Jones' Mariner 9 analyses has not been attempted using Viking data.

Preservational information from *Barlow* [1987b], derived from analysis of the Viking 1:2,000,000 photomosaics, is used in this study to determine the existence and time of cessation of erosional episodes on Mars during the heavy bombardment period. The catalog used here contains size, location, morphology, and preservational information for 42,283 impact craters located across the entire Martian surface and is considered complete for craters ≥8 km diameter (25,826 craters). Qualitative classifications currently are used in the preservational information column of the catalog, although these data will be quantified in the near future. More thorough analyses of the timing and extent of obliterative episodes must wait until the data are quantified, but some information about the regional extent and timing of erosional periods can be obtained from the present catalog information.

Craters surrounded by a well-preserved ejecta blanket tend to display sharp rims, well-defined interior structures, and little depositional infilling of the crater floor. These features are representative of fresh impact crater morphologies and suggest that craters surrounded by pristine ejecta blankets have not been exposed to high amounts of obliteration since their formation. Relative crater size-frequency distribution curves of craters with ejecta blankets (subsequently referred
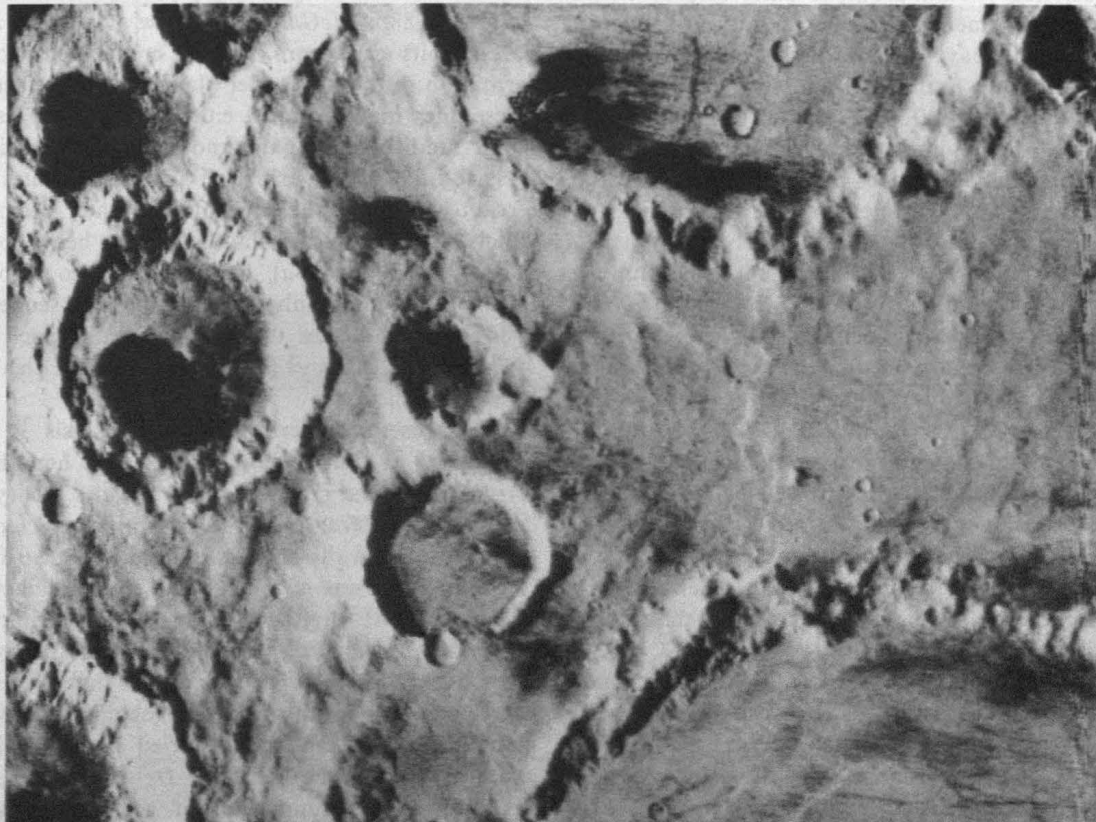


Fig. 3. Example of the degraded appearance displayed by many Martian craters located in the southern highlands. The low rims and shallow floors of most craters in this image suggest that this area has undergone a substantial amount of degradation since the formation of these craters. (Viking orbiter frame 510A46; image is 49 x 96 km.)

to as "fresh craters") provide crater densities and their relationship to the heavy bombardment period, which can be used to constrain the time of cessation of erosional periods. Distribution curves were computed for fresh craters superposed on the 25 geologic units defined by *Barlow* [1987a; 1988a]. Figure 4a shows the distribution curves of uplands, intercrater plains, and ridged plains derived from data in the catalog [*Barlow*, 1987b] and discussed by *Barlow* [1987a; 1988a]. Figure 4b shows the fresh crater curves for these same units; all show a curve shape indicative of formation during the period of heavy bombardment and all have crater density values near a log $R$ value of -2. Except for those geologic units known to have undergone obliterative processes since the end of heavy bombardment (e.g., dissected boundary material), all heavy bombardment aged units show a clustering of fresh crater size-frequency distribution curves near the log $R$ value of -2, approximately equivalent in crater density to that of the total ridged plains curve. The results suggest that although localized regions have undergone varying amounts of erosion, most heavy bombardment aged units show a consistent termination of ejecta obliteration at about the same time as ridged plains formation, near the end of heavy bombardment. In addition, the shape of the fresh crater curves supports our earlier argument that erosion is not the primary cause of the multisloped distribution curve.

An alternate means of determining the amount of obliteration a terrain has experienced is to compute the ratio of fresh crater density to normal crater density. Table 2 shows the results of these calculations for each geologic unit defined by *Barlow* [1987a, 1988a]. Those units of heavy bombardment age consistently show much lower ratios than end of heavy bombardment and post-heavy bombardment aged units. Most heavy bombardment units display ratios between 0.16 and 0.26 (mean = 0.206, maximum difference = 0.10), while end of heavy bombardment and post-heavy bombardment units have ratios in the range 0.64 to 0.75 (mean = 0.695, maximum difference = 0.11). Computation of the density ratio over regions of more limited areal extent shows a larger range in ratio values per terrain unit, but the general trend of heavy bombardment aged units having low values (ratios generally less than 0.35) and end of heavy bombardment and post-heavy bombardment units having high values (ratios predominantly greater than 0.50) is still evident. If obliteration rates had been constant over Martian history, we would observe a gradual decrease in ratio value with increasing age. The observation that the ratio values drop significantly prior to the cessation of heavy bombardment suggests that an areally extensive episode of obliteration with rates higher than those at present existed prior to the end of heavy bombardment. Localized regions across Mars have undergone varying amounts of obliteration throughout time, but the last (and possibly only) areally extensive high obliteration episode ended during the time when the impact flux was still relatively high.

Many studies have found that high obliteration rates ceased early in Martian history, but the relationship between this period of obliteration and the end of heavy bombardment has been a source of controversy [*Soderblom et al.*, 1974; *Chapman*, 1974; *Jones*, 1974]. Based on the shapes and densities of the fresh crater size-frequency distribution curves, this study proposes that the period of high obliteration rates terminated during the declining stages of the period of heavy

bombardment, around the time of the ridged plains formation. This time period correlates not only with decreasing impact flux but also with a major change in volcanic style from predominantly simple flows to more complex flows and volcanic constructs [*Greeley and Spudis*, 1981] and with a possible change in atmospheric conditions as deduced from geologic features in the Argyre Basin region [*Schultz*, 1986]. The degree to which each of these processes contributed to the obliteration rate is unknown and require continued study to determine the beginning and extent of the period of high obliteration rates.

## CRUSTAL DICHOTOMY

The differences in age and elevation between the northern and southern hemispheres on Mars were first noted in Mariner 9 images and have been more thoroughly investigated using Viking orbiter data. Currently, three major theories of the dichotomy formation exist: internal processes [*Wise et al.*, 1979; *Phillips*, 1988; *Turcotte*, 1988], single megaimpact [*Wilhelms and Squyres*, 1984], and multiple basin size impacts [*Frey et al.*, 1986; *Frey and Schultz*, 1988a,b]. The model proposing an internal origin for the dichotomy is best addressed from geophysical analyses rather than cratering arguments and will not be addressed here. The megaimpact model, in which much of the northern hemisphere constitutes the floor of a 7700-km-diameter crater called the Borealis Basin, is proposed to have occurred early in Martian history, prior to the formation of most if not all of the Martian surface units retained today. The cratering record can only provide constraints on the maximum relative age of the units superposed on this proposed basin, thus providing the latest time at which the impact could have occurred. Crater size-frequency distribution analysis of the knobby terrain (Figure 5) [*Maxwell and McGill*, 1988; *Barlow*, 1988b; *McGill*, 1988] show a range of ages, but the oldest units are approximately contemporaneous with the formation of the intercrater plains in the southern highlands. These ages may represent either formation ages or times of major modification of the knobby terrain, but in either case the size-frequency distribution analysis indicates that knobby terrain existed at the time of intercrater plains formation, which dates from the middle of the heavy bombardment period [*Barlow*, 1988a], or the Middle to Upper Noachian on the more commonly used stratigraphic sequence [*Tanaka*, 1986]. This indicates that the gigantic impact proposed by *Wilhelms and Squyres* [1984] must predate this early period in Martian history.

The present cratering record analysis is particularly applicable to the testing of the third hypothesis for the formation of the crustal dichotomy, the theory of multiple large impacts [*Frey et al.*, 1986; *Frey and Schultz*, 1988a,b]. It is known that the crater size-frequency distribution curves for Martian basins in the 100 to 800-km-diameter range lies below that of the Moon in the same diameter range, indicating a paucity of Martian basins [cf. *Strom et al.*, 1990]. The multiple-basin hypothesis argues that the discrepancy of Martian basins results from the inability of investigators to identify severely eroded or buried basins. This hypothesis assumes that basins follow a $D^{-2}$ production function, as suggested by extrapolation of the cumulative curve for smaller craters. The proponents of this theory argue that the Borealis Basin does not exist because too many basins are "missing" if the Borealis Basin is the largest member of the
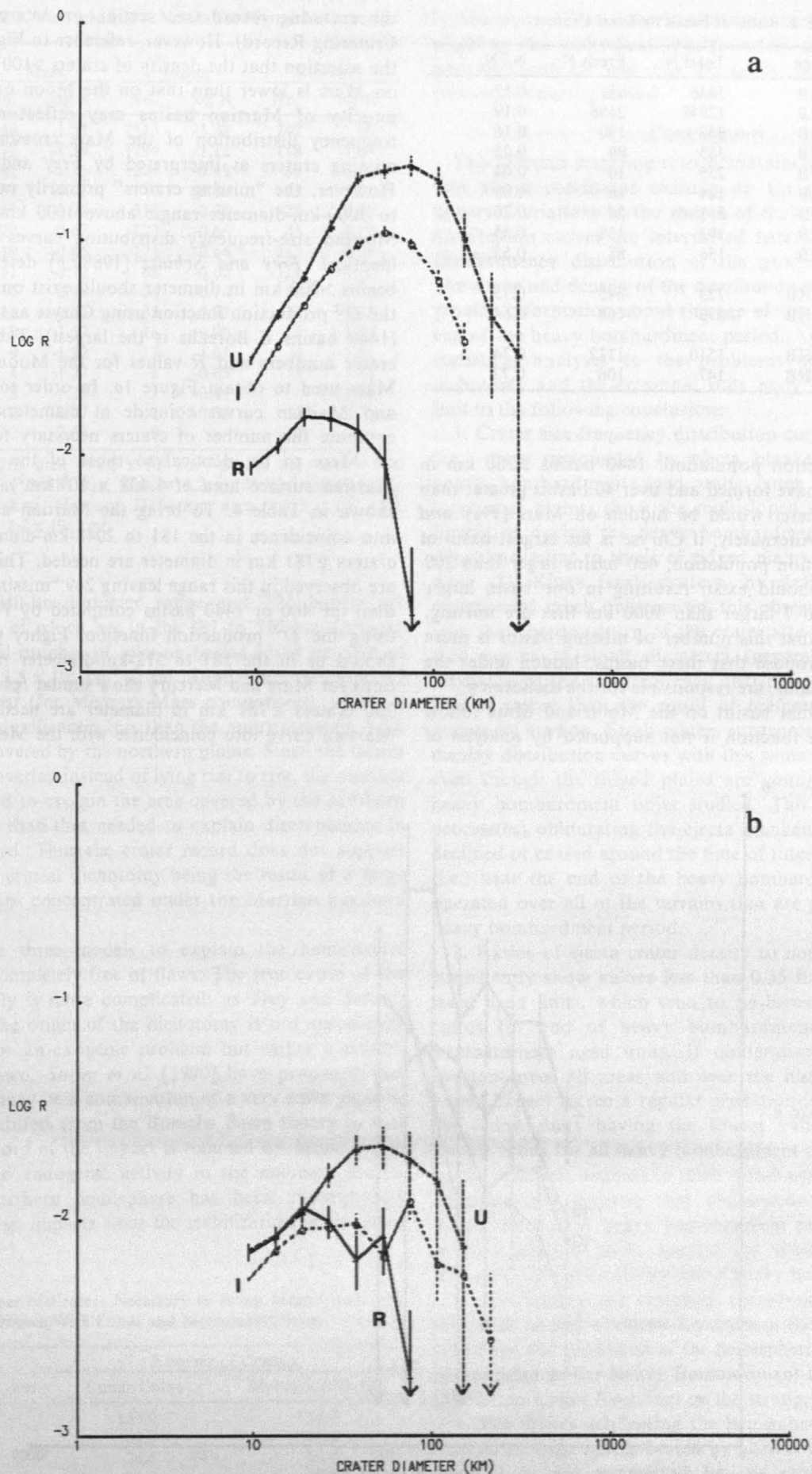
Fig. 4. Relative crater size-frequency distribution plots of (a) all craters (except those almost completely buried by overlying deposits) superposed on the Martian uplands (U), intercrater plains (I), and ridged plains (R), and (b) craters displaying pristine ejecta blankets superposed on the uplands (U), intercrater plains (I), and ridged plains (R).

TABLE 2. Ratio of Fresh to Total Craters

| Unit | Age | Total N | Fresh N | $N_f/N_t$ |
|------|-----|---------|---------|-----------|
| Uplands | HB | 3636 | 631 | 0.17 |
| Intercrater plains | HB | 12849 | 2456 | 0.19 |
| Mountain | HB | 807 | 130 | 0.16 |
| Fractured uplands | HB | 355 | 89 | 0.25 |
| Fretted | HB | 235 | 10 | 0.04 |
| Exhumed | HB | 124 | 10 | 0.08 |
| Dissected | HB | 337 | 86 | 0.26 |
| Knobby | HB | 393 | 138 | 0.35 |
| Hellas volcanic plains | HB | 156 | 85 | 0.55 |
| Ridged | EHB | 723 | 545 | 0.75 |
| Cratered and fractured plains | PHB | 273 | 168 | 0.64 |
| Plains | PHB | 1510 | 1112 | 0.74 |
| Volcanic plains | PHB | 147 | 106 | 0.72 |

$D^{-2}$ basin production population: 1440 basins >200 km in diameter should have formed and over 40 basins greater than 1000 km in diameter would be hidden on Mars [*Frey and Schultz*, 1988b]. Alternately, if Chryse is the largest basin of this same production population, 460 basins larger than 200 km in diameter should exist, resulting in one basin larger than 2000 km and 7 larger than 1000 km that are missing. The authors feel that this number of missing basins is more reasonable and propose that these basins, hidden under the young northern plains, are responsible for the dichotomy.

The argument that basins on the Moon and Mars follow a $D^{-2}$ distribution function is not supported by analysis of the cratering record (see section on Interpretation of the Cratering Record). However, reference to Figure 1a supports the assertion that the density of craters >100 km in diameter on Mars is lower than that on the Moon or Mercury. This paucity of Martian basins may reflect either the size-frequency distribution of the Mars crossing impactors or missing craters as interpreted by Frey and his colleagues. However, the "missing craters" primarily occur in the 128- to 1000-km-diameter range: above 1000 km, the lunar and Martian size-frequency distribution curves are statistically identical. *Frey and Schultz* [1988a,b] determine that 460 basins >200 km in diameter should exist on Mars based on the $D^{-2}$ production function using Chryse as the largest crater (1440 basins if Borealis is the largest). Table 3 shows the crater numbers and $R$ values for the Moon, Mercury, and Mars used to obtain Figure 1a. In order to have the lunar and Martian curves coincide at diameters >150 km, we compute the number of craters necessary for the $R$ values on Mars to be identical to those of the Moon (using a Martian surface area of $1.438 \times 10^8$ km$^2$). The results are shown in Table 4. To bring the Martian and lunar curves into coincidence in the 181 to 2048-km-diameter range, 287 craters $\geq 181$ km in diameter are needed. Thirty-eight craters are observed in this range leaving 249 "missing basins" rather than the 460 or 1440 basins computed by Frey and Schultz using the $D^{-2}$ production function. Eighty percent of these should be in the 181 to 512-km-diameter range. Computations for Mars and Mercury show similar results. In this case, 260 craters $\geq 181$ km in diameter are needed to bring the Martian curve into coincidence with the Mercurian curve in
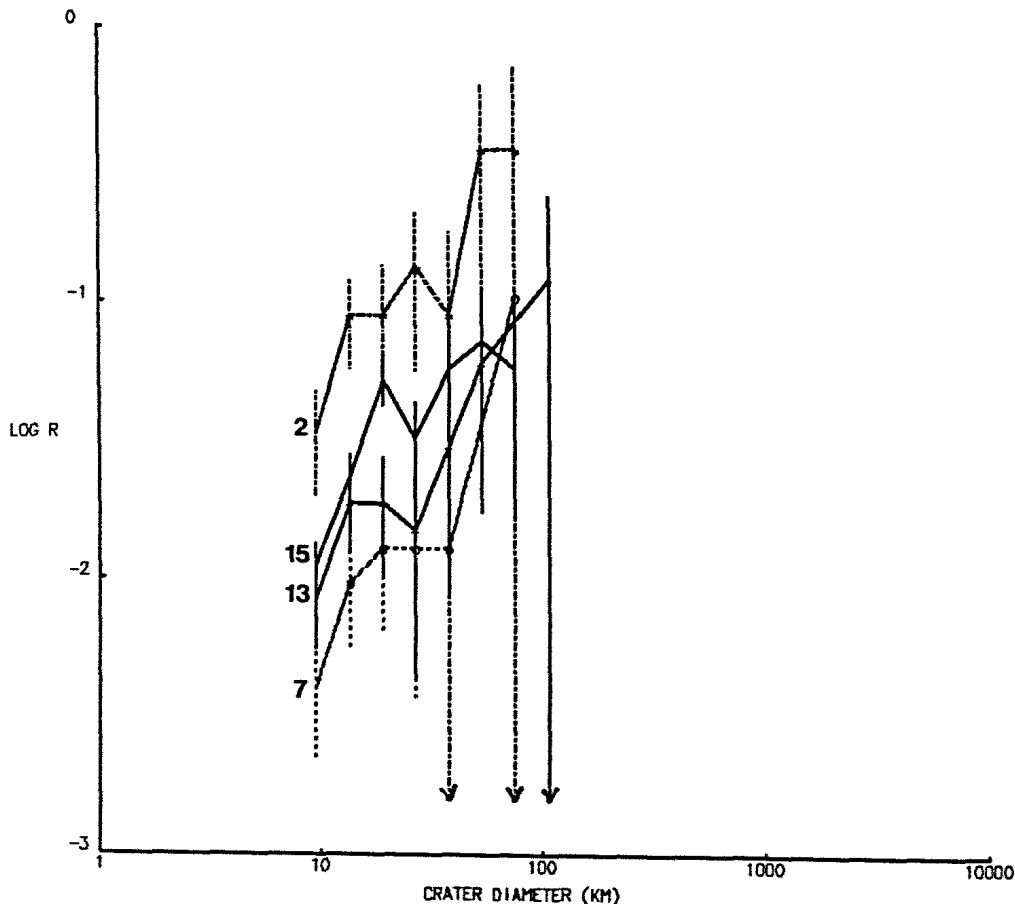


Fig. 5. Relative crater size-frequency distribution plots of the knobby terrain in quadrangles MC02, MC07, MC13, and MC15. Crater densities of the knobby terrain indicate a range of formation ages throughout the span of the heavy bombardment period.

TABLE 3. Numbers and R Values for Figure 2a

| Mean Diameter, km | Mars | | Moon | | Mercury | |
|---|---|---|---|---|---|---|
| | No. | log R | No. | log R | No. | log R |
| 9.51 | 946 | -1.55 | 2515 | -1.28 | 242 | -1.60 |
| 13.45 | 777 | -1.34 | 1794 | -1.12 | 118 | -1.61 |
| 19.03 | 582 | -1.16 | 1204 | -0.99 | 88 | -1.44 |
| 26.91 | 499 | -0.93 | 777 | -0.88 | 72 | -1.22 |
| 38.05 | 417 | -0.71 | 510 | -0.76 | 75 | -0.90 |
| 53.82 | 227 | -0.67 | 323 | -0.66 | 45 | -0.82 |
| 76.11 | 119 | -0.65 | 171 | -0.64 | 217 | -0.78 |
| 107.63 | 51 | -0.72 | 88 | -0.62 | 128 | -0.70 |
| 152.22 | 14 | -0.98 | 34 | -0.74 | 56 | -0.76 |
| 215.27 | 11 | -1.74 | 35 | -0.91 | 23 | -0.85 |
| 304.44 | 8 | -1.57 | 18 | -0.90 | 7 | -1.06 |
| 430.54 | 9 | -1.22 | 7 | -1.01 | 4 | -1.01 |
| 608.87 | 4 | -1.27 | 8 | -0.65 | 3 | -0.83 |
| 861.10 | 2 | -1.27 | 7 | -0.41 | 1 | -1.01 |
| 1217.75 | 2 | -0.97 | 1 | -0.95 | 1 | -0.70 |
| 1722.21 | 2 | -0.67 | 0 | — | 0 | — |

Mars: $D<181$ km, area $= 8.8 \times 10^6$ km$^2$; $D>181$ km, area $= 8.0 \times 10^7$ km$^2$. Moon: $D<181$ km, area $= 1.2 \times 10^8$ km$^2$; $D>181$ km, area $= 3.8 \times 10^7$ km$^2$. Mercury: $D<64$ km, area $= 2.5 \times 10^6$ km$^2$; $D>64$ km, area $= 2.2 \times 10^7$ km$^2$.

the 181 to 2048-km-diameter range and 221 basins are "missing", 87% of which are in the 181 to 512-km-diameter range. The total number of missing basins cover an area of approximately $3.5 \times 10^7$ km$^2$ (from Moon-Mars comparison) or $2.6 \times 10^7$ km$^2$ (for Mercury-Mars comparison), which is similar to but significantly less than the approximately $5.5 \times 10^7$ km$^2$ area covered by the northern plains. Since the basins would tend to overlap instead of lying rim to rim, the number of basins needed to explain the area covered by the northern plains is larger than that needed to explain discrepancies in the crater record. Thus the crater record does not support the idea of the crustal dichotomy being the result of a large number of basins concentrated under the Martian northern plains material.

None of the three models to explain the hemispheric dichotomy is completely free of flaws. The true cause of the dichotomy likely is more complicated: as *Frey and Schultz* [1988b] note, the origin of the dichotomy is not specifically an endogenic or an exogenic problem but rather a combination of the two. *Strom et al.* [1990] have proposed that the dichotomy may be a combination of a very early gigantic impact (which differs from the Borealis Basin theory in that no geologic record of the impact is retained on Mars) which led to enhanced endogenic activity in the northern hemisphere. The northern hemisphere has been subsequently modified by large impacts since the stabilization of the crust

TABLE 4. Number of Craters Necessary to Bring Mars Curve Into Concurrence With Lunar and Mercurian Curves

| Mean Diameter, km | Number of Craters | |
|---|---|---|
| | Lunar Curve | Mercurian Curve |
| 215.27 | 133.0 | 152.7 |
| 304.44 | 68.0 | 47.1 |
| 430.53 | 26.4 | 26.4 |
| 608.87 | 30.2 | 20.0 |
| 861.10 | 26.3 | 6.7 |
| 1217.75 | 3.8 | 6.7 |
| Total | 287.7 | 259.6 |

in this region. This scenario eliminates many of the problems plaguing the individual models while incorporating their positive qualities and can be easily reconciled with the observed cratering record.

## CONCLUSIONS

The Martian cratering record contains important information about conditions existing on the planet early in its history. Variations in the shapes of the crater size-frequency distribution curves are interpreted here as indicative of the size-frequency distribution of the production populations. The shape and density of the distribution curves can therefore provide information about the age of the unit relative to the end of the heavy bombardment period. Application of crater statistical analyses to the problems of the hemispheric dichotomy and the erosional state early in Martian history lead to the following conclusions:

1. Crater size-frequency distribution curves of fresh craters (i.e., those surrounded by ejecta blankets) superposed on heavy bombardment aged units (such as the highlands intercrater plains) show the multisloped shape indicative of formation during the heavy bombardment period but with densities similar to those of ridged plains areas (log R value near -2). Since fresh craters, by definition, have not experienced much obliteration, this observation supports the idea that the downturn of the crater size-frequency distribution curves at small diameters (generally <70 km) is a reflection of the size-frequency distribution of the impacting objects rather than the result of preferential loss of small craters by erosion. Fresh craters superposed on ridged plains display distribution curves with this same shape and density, even though the ridged plains are younger than the other heavy bombardment units studied. This suggests that the process(es) obliterating the ejecta blankets of impact craters declined or ceased around the time of ridged plains formation (i.e., near the end of the heavy bombardment period) and operated over all of the terrains that are preserved from the heavy bombardment period.

2. Ratios of ejecta crater density to normal crater density consistently show values less than 0.35 for heavy bombardment aged units, which tend to be lower than the average ratios for end of heavy bombardment and post-heavy bombardment aged units. If obliteration rates have been constant over all areas and over the history of Mars, one would expect to see a regular gradation in these ratios with the oldest units having the lowest values. The observed similar ratios for all heavy bombardment aged units followed by the dramatic increase in ratio values near the end of heavy bombardment suggests that obliteration rates were much higher during the heavy bombardment period and dropped to their present levels around the time of ridged plains formation just prior to the end of heavy bombardment.

3. Analysis of the cratering record on the oldest units preserved in the northern hemisphere (i.e., knobby terrain) constrains the formation of the hemispheric dichotomy to the period prior to the Heavy Bombardment-Intermediate epoch (Middle to Upper Noachian on the stratigraphic scale).

4. The theory attributing the hemispheric dichotomy to a number of large basins buried by northern hemisphere plains deposits is not supported by the crater size-frequency distribution data. The crater size-frequency distribution curves of heavily cratered units do not follow a power law distribution function with incremental slope -2 at all crater

diameters. The use of this presumed distribution overestimates the number of "missing" basins on Mars compared to the lunar and Mercurian distribution curves. The corrected values result in too few basins to account adequately for the area covered by northern plains.

These results from the analysis of craters superposed on heavily cratered units across the Martian surface provide further constraints on the problems of the hemispheric dichotomy and early erosional conditions on Mars. Although crater analyses have been used extensively to infer the geologic history of the northern hemisphere of the planet, similar analyses thus far have been used in only a cursory fashion for much of the older southern hemisphere. That trend is beginning to change as interest in early Martian conditions increases [*Tanaka et al.*, 1988; *Schultz*, 1988]. Further statistical study of craters in various stages of preservation and displaying a variety of morphologies promises to dramatically broaden our understanding of the forces which have shaped the Martian surface into what we see today.

## REFERENCES

Barlow, N.G., Relative ages and the geologic evolution of Martian terrain units, Ph.D. thesis, Univ. of Ariz., Tucson, 1987a.

Barlow, N.G., Catalog of large martian impact craters, Submitted as NASA Contractor Report, 1987b.

Barlow, N.G., Crater size-frequency distributions and a revised martian relative chronology, *Icarus, 75,* 285-305, 1988a.

Barlow, N.G., Conditions on early Mars: Constraints from the cratering record, MEVTV Workshop on Early Tectonic and Volcanic Evolution of Mars, *LPI Tech. Rep. 89-04,* pp. 15-16, Lunar and Planet. Inst., Houston, Tex., 1989.

Basaltic Volcanism Study Project, *Basaltic Volcanism on the Terrestrial Planets,* Pergamon, New York, 1981.

Chapman, C.R., Cratering on Mars, I, Cratering and obliteration history, *Icarus, 22,* 272-291, 1974.

Chapman, C.R., and K.L. Jones, Cratering and obliteration history of Mars, *Annu. Rev. Earth Planet. Sci., 5,* 515-540, 1977.

Chapman, C.R., and W.B. McKinnon, Cratering of planetary satellites, in *Satellites,* edited by J. Burns and M.S. Matthews, pp. 492-580, University of Arizona Press, Tucson, 1986.

Chapman, C.R., J.B. Pollack, and C. Sagan, An analysis of the Mariner 4 cratering statistics, *Astron. J., 74,* 1039-1051, 1969.

Crater Analysis Techniques Working Group, Standard techniques for presentation and analysis of crater size-frequency data, *NASA Tech. Memo. TM-79730,* 1978.

Frey, H. and R.A. Schultz, Large impact basins and the megaimpact origin for the crustal dichotomy on Mars, *Geophys. Res. Lett., 15,* 229-232, 1988a.

Frey, H. and R.A. Schultz, Origin of the Martian crustal dichotomy, MEVTV Workshop on Early Tectonic and Volcanic Evolution of Mars, *LPI Tech. Rep. 89-04,* pp. 35-37, Lunar and Planet. Inst., Houston, Tex, 1989.

Frey, H.V., R.A. Schultz, and T.A. Maxwell, The Martian crustal dichotomy: Product of accretion and not a specific event?, *Lunar Planet. Sci., XVII,* 241-242, 1986.

Frey, H.V., A.M. Semeniuk, J.A. Semeniuk, and S. Tokarcik, A widespread common age resurfacing event in the highlands-lowland transition zone in eastern Mars, *Proc. Lunar Planet. Sci. Conf., 18th,* 679-699, 1988.

Greeley, R., and P.D. Spudis, Volcanism on Mars, *Rev. Geophys. Space Phys., 19,* 13-41, 1981.

Hartmann, W.K., Martian cratering,II, Asteroid impact history, *Icarus, 15,* 396-409, 1971.

Hartmann, W.K., Martian cratering, 4, Mariner 9 initial analysis of cratering chronology, *J. Geophys. Res., 78,* 4096-4116, 1973.

Hartmann, W.K., Does crater "saturation equilibrium" occur in the solar system?, *Icarus, 60,* 56-74, 1984.

Jones, K.L., Evidence for an episode of crater obliteration intermediate in martian history, *J. Geophys. Res., 79,* 3917-3931, 1974.

Maxwell, T.A., and G.E. McGill, Ages of fracturing and resurfacing in the Amenthes Region, Mars, *Proc. Lunar Planet. Sci. Conf., 18th,* 701-711, 1988.

McGill, G.E., The Martian crustal dichotomy, MEVTV Workshop on Early Tectonic and Volcanic Evolution of Mars, *LPI Tech. Rep. 89-04,* pp. 59-61, Lunar and Planet. Inst., Houston, TX, 1989.

McGill, G.E., and D.U. Wise, Regional variations in degradation and density of martian craters, *J. Geophys. Res., 77,* 2433-2441, 1972.

Murray, B.C., L.A. Soderblom, R.P. Sharp, and J.A. Cutts, The surface of Mars, 1, Cratered terrains, *J. Geophys. Res., 76,* 313-330, 1971.

Neukum, G., On the question of cratering equilibrium vs production populations, *Lunar Planet. Sci., XVI,* 614-615, 1985.

Neukum, G., and K. Hiller, Martian ages, *J. Geophys. Res., 86,* 3097-3121, 1981.

Neukum, G., and D.U. Wise, Mars: A standard crater curve and possible new time scale, *Science, 194,* 1381-1387, 1976.

Oberbeck, V.R., W.L. Quaide, R.E. Arvidson, and H.R. Aggarwal, Comparative studies of lunar, Martian, and Mercurian craters and plains, *J. Geophys. Res., 82,* 1681-1698, 1977.

Öpik, E.J., The Martian surface, *Science, 153,* 255-265, 1966.

Phillips, R.J., The geophysical signal of the Martian global dichotomy, *Eos Trans. AGU, 69,* 389, 1988.

Pollack, J.B., J.F. Kasting, S.M. Richardson, and K. Poliakoff, The case for a wet, warm climate on early Mars, *Icarus, 71,* 203-224, 1987.

Sagan, C., O.B. Toon, and P.J. Gierasch, Climatic change on Mars, *Science, 181,* 1045-1049, 1973.

Schultz, P.H., The Martian atmosphere before and after the Argyre impact, Reports of the Planetary Geology and Geophysics Program 1985, *NASA Tech. Memo. TM-88383,* 188-189, 1986.

Schultz, P.H., Early cratering rates and the nature of the martian cratered uplands, in MEVTV Workshop on Nature and Composition of Surface Units on Mars, *LPI Tech. Rep. 88-05,* pp. 117-119, Lunar and Planet. Inst., Houston, Tex, 1988.

Soderblom, L.A., C.D. Condit, R.A. West, B.M. Herman, and T.J. Kreidler, Martian planetwide crater distributions: Implications for geologic history and surface processes, *Icarus, 22,* 239-263, 1974.

Squyres, S.W. and M.H. Carr, Geomorphic evidence for the distribution of ground ice on Mars, *Science, 231,* 249-252, 1986.

Strom, R.G., Origin and relative ages of lunar and Mercurian intercrater plains, *Phys. Earth Planet. Int., 15,* 156-172, 1977.

Strom, R.G., and E.A. Whitaker, Populations of impacting bodies in the inner solar system, Reports of the Accomplishments of the Planetary Program 1975-1976, *NASA Tech. Memo., TM-X3364,* 194-196, 1976.

Strom, R.G., S.K. Croft, and N.G. Barlow, The Martian impact cratering record, in *Mars,* University of Arizona Press, Tucson, in press, 1990.

Tanaka, K.L., The stratigraphy of Mars, *Proc. Lunar Planet. Sci. Conf., 17th,* Part 1, *J. Geophys. Res., 91,* Supp., E139-E158, 1986.

Tanaka, K.L., N.K. Isbell, D.H. Scott, R. Greeley, and J.E. Guest, The resurfacing history of Mars: A synthesis of digitized, Viking-based geology, *Proc. Lunar Planet. Sci. Conf., 18th,* 665-678, 1988.

Turcotte, D.L., Early evolution of the Martian interior, *Eos Trans. AGU, 69,* 389, 1988.

Wilhelms, D.E., and S.W. Squyres, The Martian hemispheric dichotomy may be due to a giant impact, *Nature, 309,* 138-140, 1984.

Wise, D.U., M.P. Golombek, and G.E. McGill, Tharsis Province, Mars: Geologic sequence, geometry, and a deformation mechanism, *Icarus, 38,* 456-472, 1979.

Woronow, A., Crater saturation and equilibrium: A Monte Carlo simulation, *J. Geophys. Res., 82,* 2447-2456, 1977.

Woronow, A., A general cratering-history model and its implications for the lunar highlands, *Icarus, 34,* 76-88, 1978.

Woronow, A., A Monte Carol study of parameters affecting computer simulations of crater saturation density, *Proc. Lunar Planet. Sci. Conf. 15th*, Part 2, *J. Geophys. Res., 90*, Supp., C817-C824, 1985.

Woronow, A., R.G. Strom, and M. Gurnis, Interpreting the cratering record: Mercury to Ganymede and Callisto, in *Satellites of Jupiter*, edited by D. Morrison, pp. 235-276, University of Arizona Press, Tucson, 1982.

N. G. Barlow, Mail Code SN21, NASA Johnson Space Center, Houston, TX 77058.